Electronic supplementary information

Alkali-metal coating: an effective method to inject electrons into cage molecules, and achieve direct metal-metal bonds and spherical aromaticity for endohedral metallofullerenes

Xiaojiao Gu and Peng Jin*

School of Materials Science and Engineering, Hebei University of Technology, Tianjin 300130, China. E-mail: china.peng.jin@gmail.com

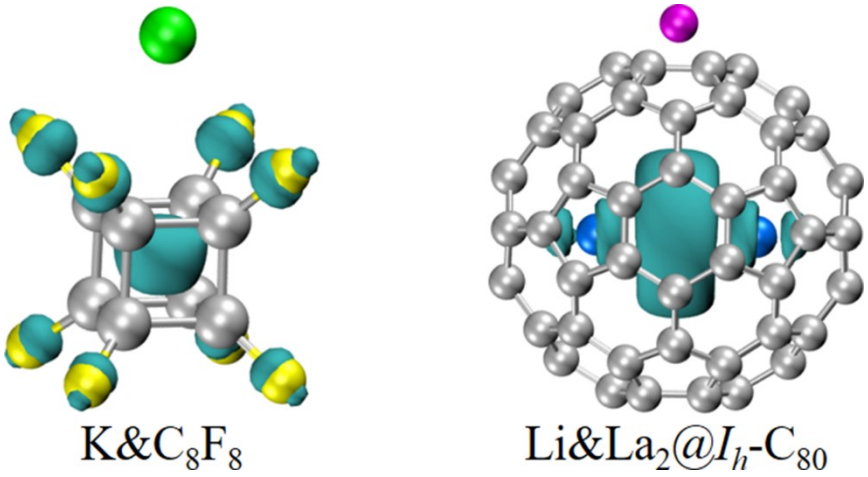

Fig. S1 Spin density distribution (reflecting the difference in the density distribution of spin-up (α) and spin-down (β) electrons) of $K\&C_8F_8$ and $Li\&La_2@C_{80}$.

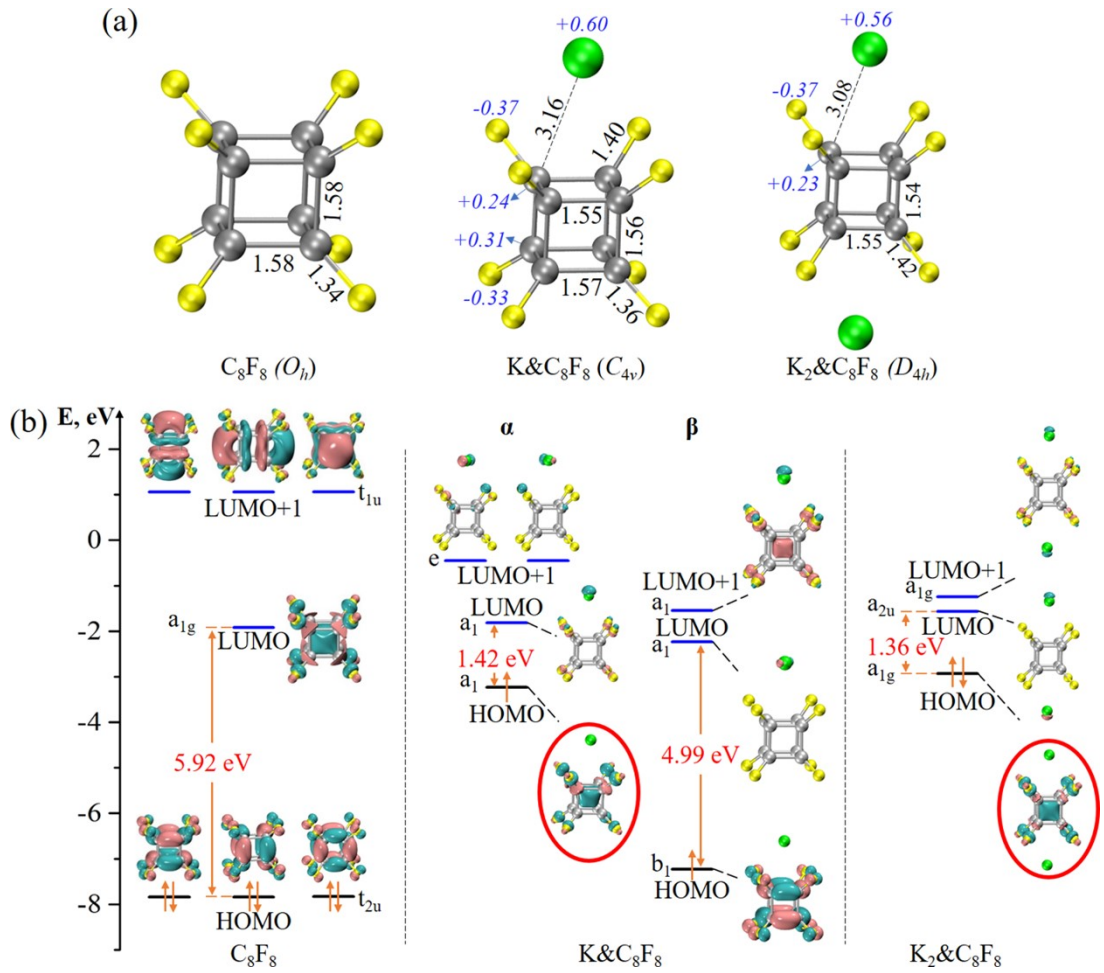

Fig. S2 (a) Optimized structures and (b) frontier molecular orbitals of C_8F_8 and K_n&C_8F_8 (n = 1, 2) at the B3LYP/6-31G*~SDD level (isovalue: ±0.055 a.u.; occupied and unoccupied orbital are black and blue lines, respectively). The distances are given in Å and the point-group symmetries are given in parentheses. The NPA charges of selected atoms are blue and italic. The orbitals with injected electrons are highlighted by red circles.

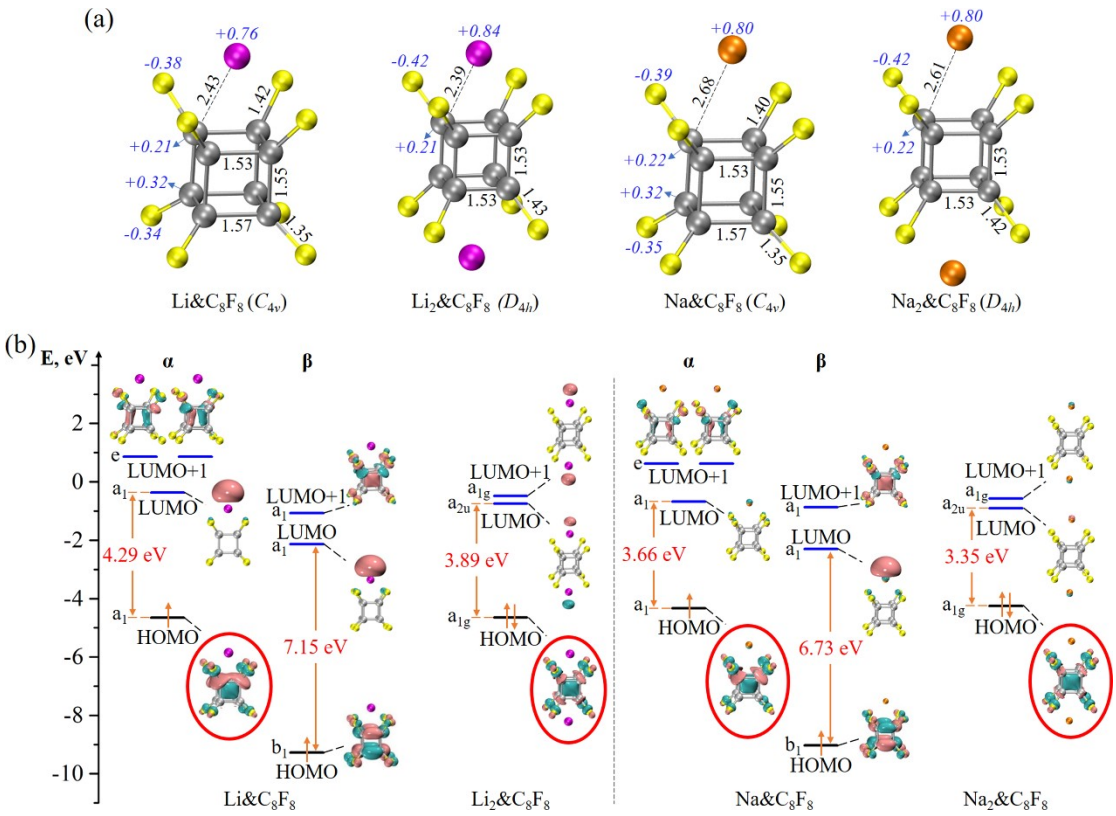

Fig. S3 (a) Optimal structures of $Li_n\&C_8F_8$ and $Na_n\&C_8F_8$ (n = 1, 2) and (b) their frontier molecular orbitals (isovalue: ±0.055 a.u.). The distances are given in Å and the point-group symmetries are given in parentheses. The NPA charges of selected atoms are blue and italic. The orbitals with injected electrons are highlighted by red circles. C: gray ball; F: yellow ball, Li: purple ball, Na: orange ball.

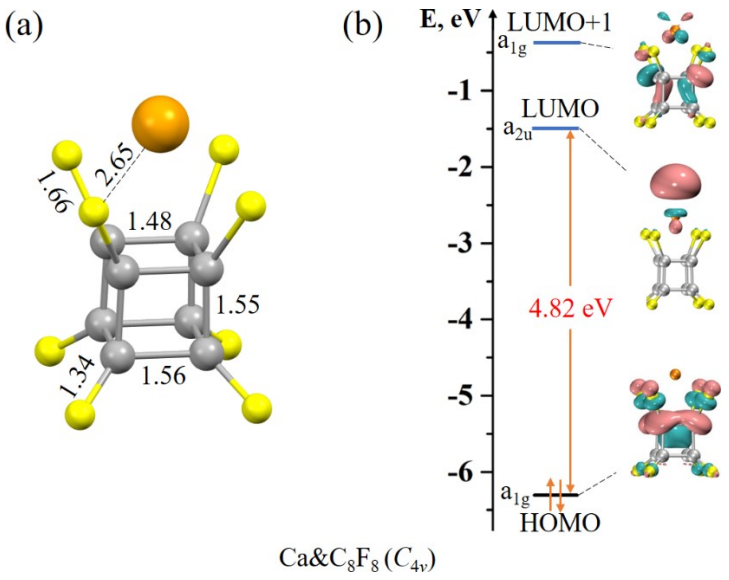

Fig. S4 (a) Optimized structure (bond length in Å) and (b) frontier molecular orbitals of $Ca\&C_8F_8$.

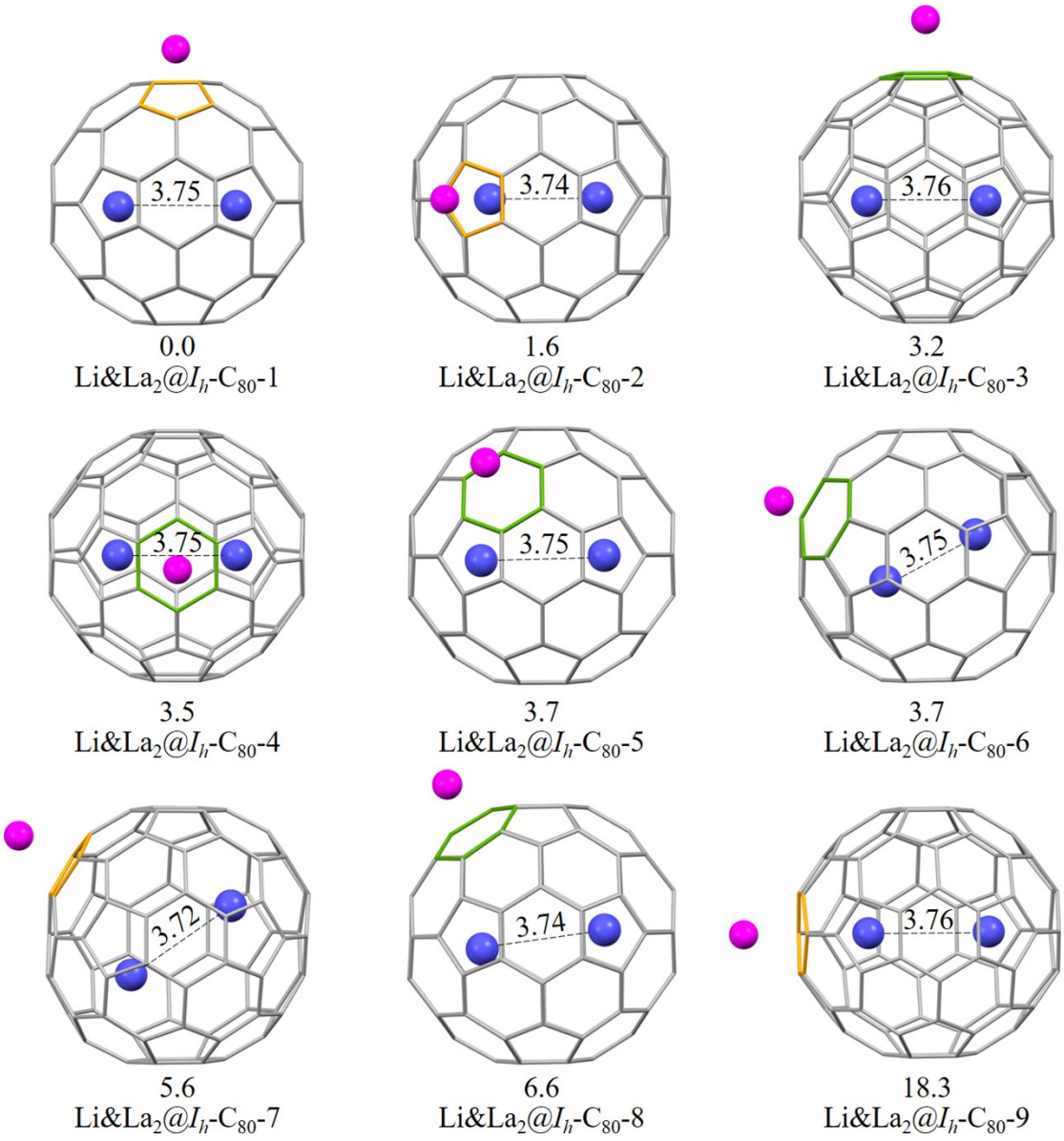

Fig. S5 Optimized structures (distance in Å) and relative energies (kcal/mol) of Li&$La_2@I_h$-C_{80} isomers with one Li atom doping on nine unequal ring positions of the $La_2@I_h$-C_{80} cage surface. The coated pentagons and hexagons are highlighted by orange and green, respectively.

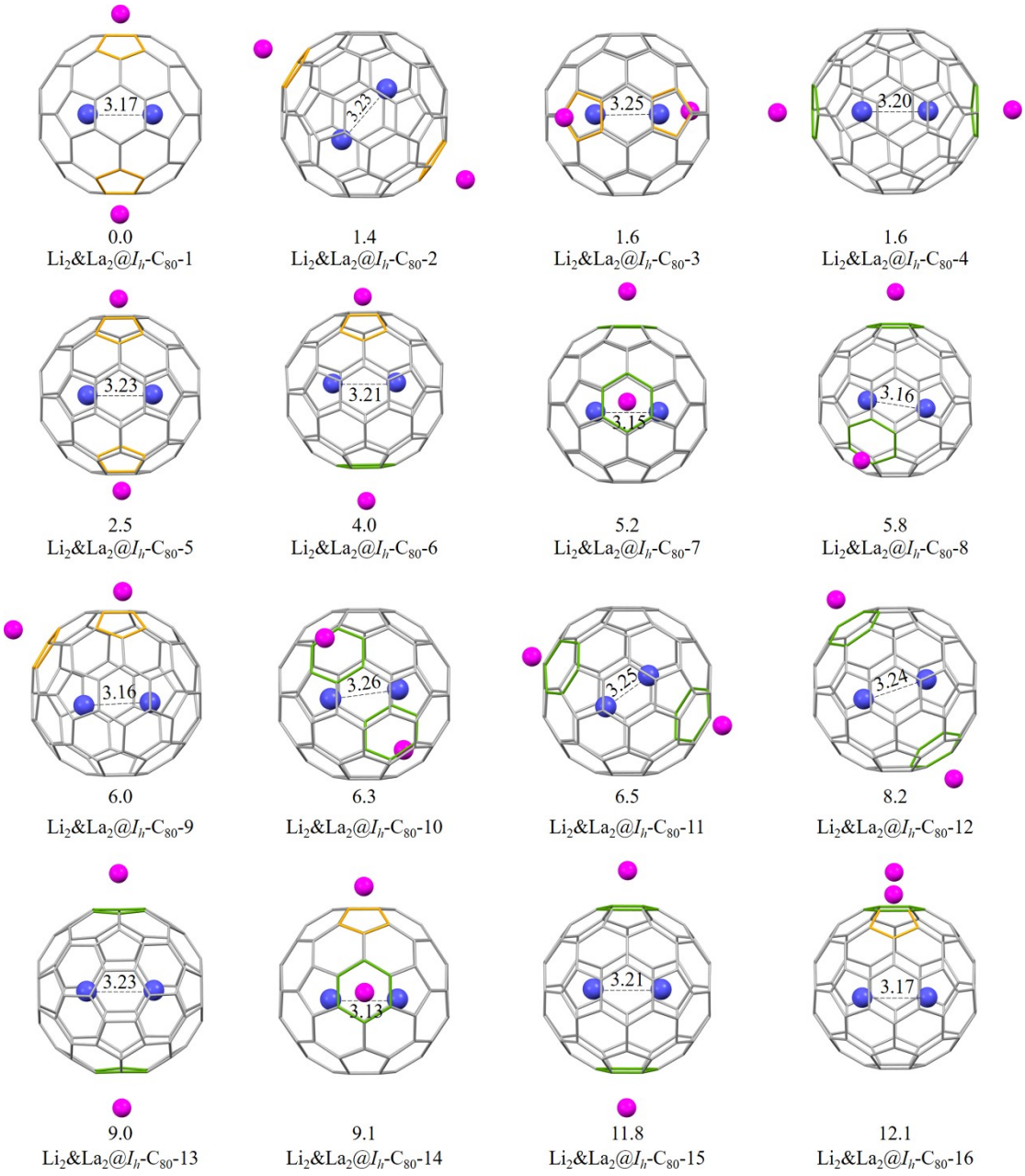

Fig. S6 Optimized structures (distance in Å) and relative energies (kcal/mol) of Li_2&La_2@I_h-C_{80} isomers with two Li atoms doping on different ring positions of the La_2@I_h-C_{80} cage surface.

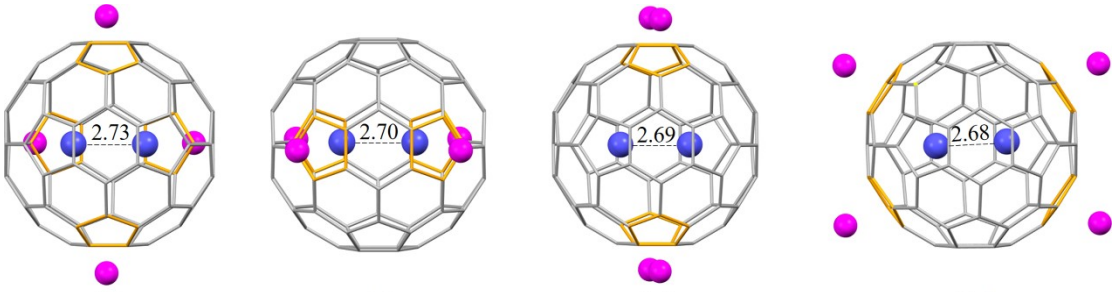

Fig. S7 Optimized structures (distance in Å) and relative energies (kcal/mol) of $Li_4\&La_2@I_h\text{-}C_{80}$ isomers with four Li atoms doping on different pentagonal ring positions of the $La_2@I_h\text{-}C_{80}$ cage surface.

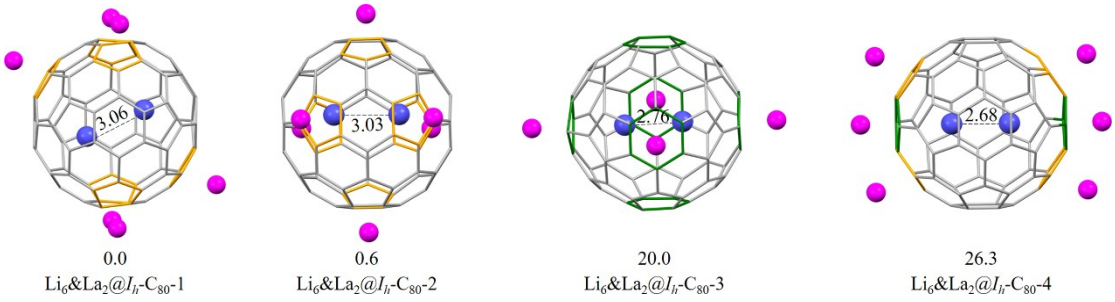

Fig. S8 Optimized structures (distance in Å) and relative energies (kcal/mol) of $Li_6\&La_2@I_h\text{-}C_{80}$ isomers with six Li atoms doping on different ring positions of the $La_2@I_h\text{-}C_{80}$ cage surface. We also considered some isomers with Li doping at hexagons to fully investigate the complex bonding situations of $Li_6\&La_2@I_h\text{-}C_{80}$ although they are obviously much higher in energy.

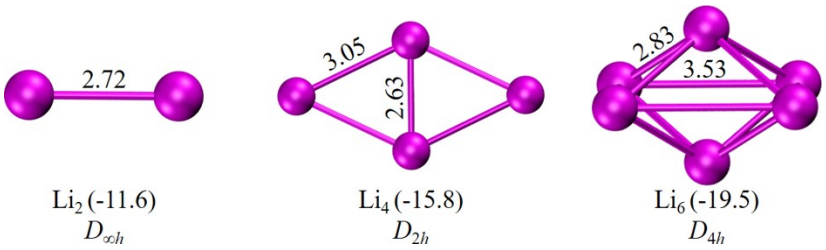

Fig. S9 Optimized structures with selected distances (Å) and cohesive energies per Li atom (kcal/mol, in parentheses) of isolated Li_n (n = 2, 4, 6) clusters. The cohesive energy per metal is calculated as $E_{coh} = (E_{Lin} - nE_{Li})/n$, where E_{Lin} and E_{Li} are the total energies of the cluster and an isolated Li atom, respectively.

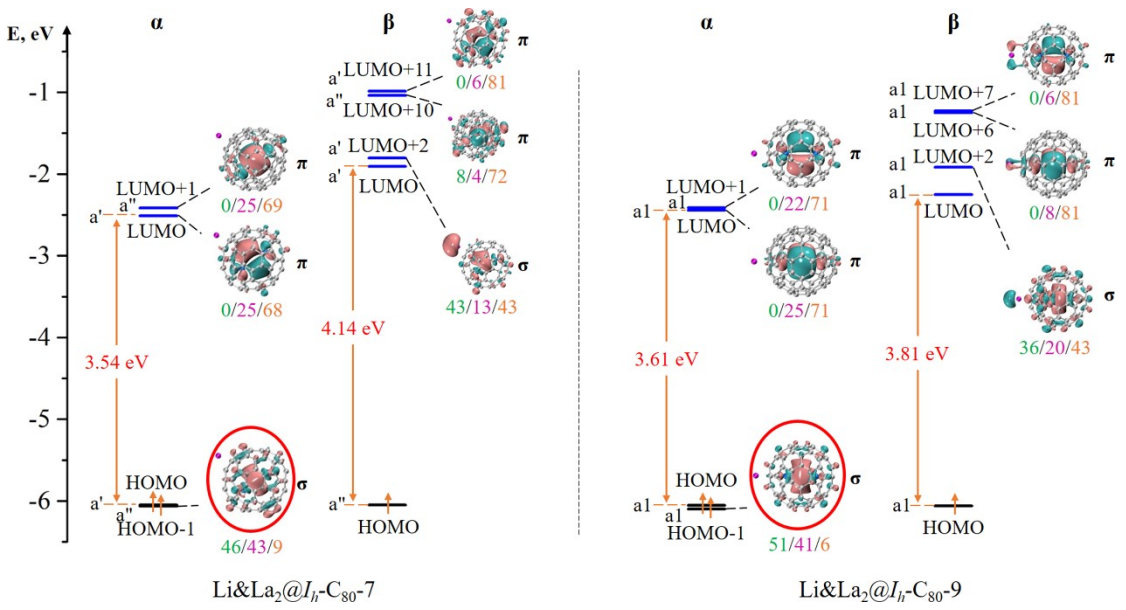

Fig. S10 La-La bonding molecular orbitals of the higher-energy isomers 7 and 9 of Li&La_2@I_h-C_{80} in Fig. S5 (isovalue: ±0.02 a.u.; occupied and unoccupied orbitals are denoted by black and blue lines, respectively).

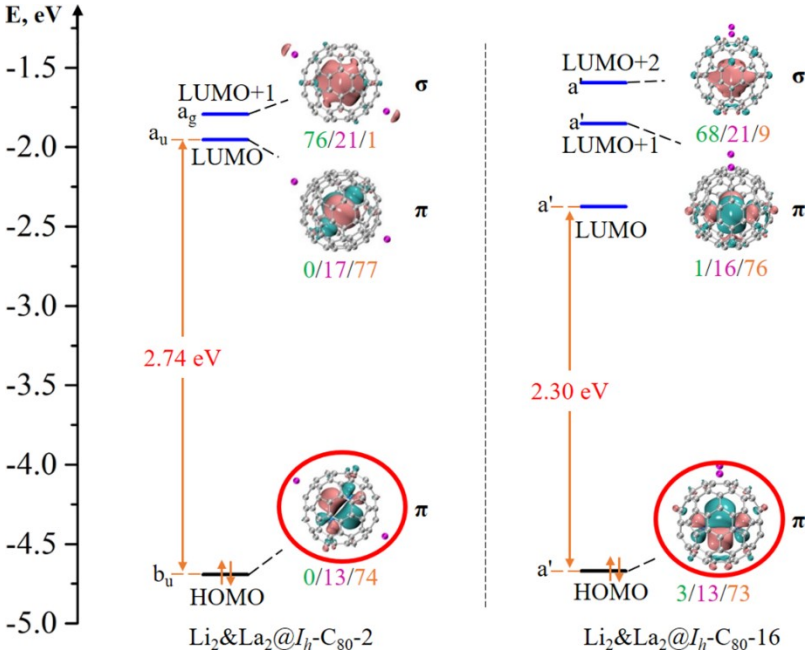

Fig. S11 La-La bonding molecular orbitals of the higher-energy isomers 2 and 16 of Li_2&La_2@I_h-C_{80} in Fig. S6 (isovalue: ±0.02 a.u.; occupied and unoccupied orbitals are denoted by black and blue lines, respectively).

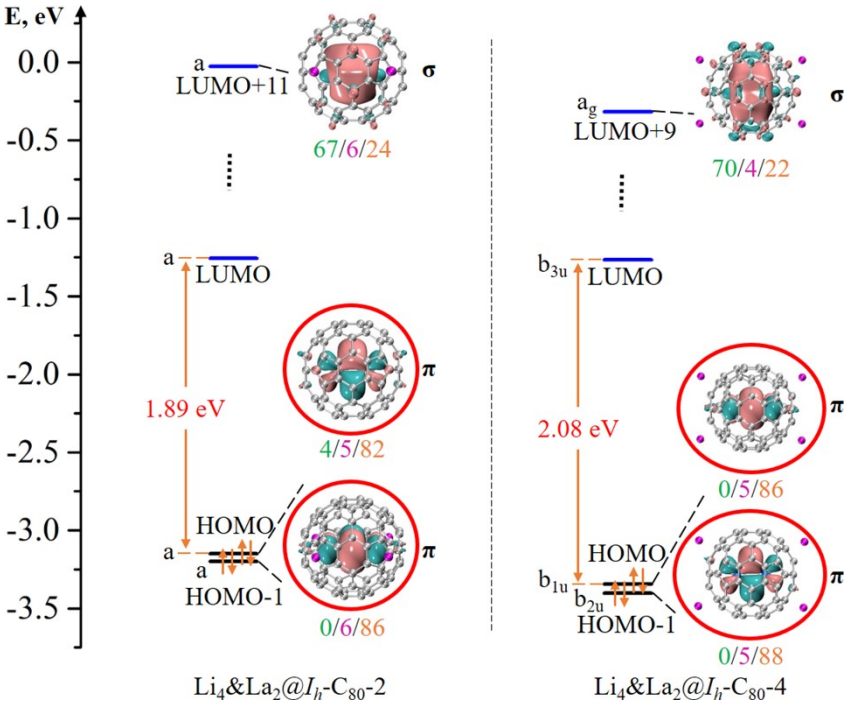

Fig. S12 La-La bonding molecular orbitals of the higher-energy isomers 2 and 4 of $Li_4\&La_2@I_h\text{-}C_{80}$ in Fig. S7 (isovalue: ±0.02 a.u.; occupied and unoccupied orbitals are denoted by black and blue lines, respectively).

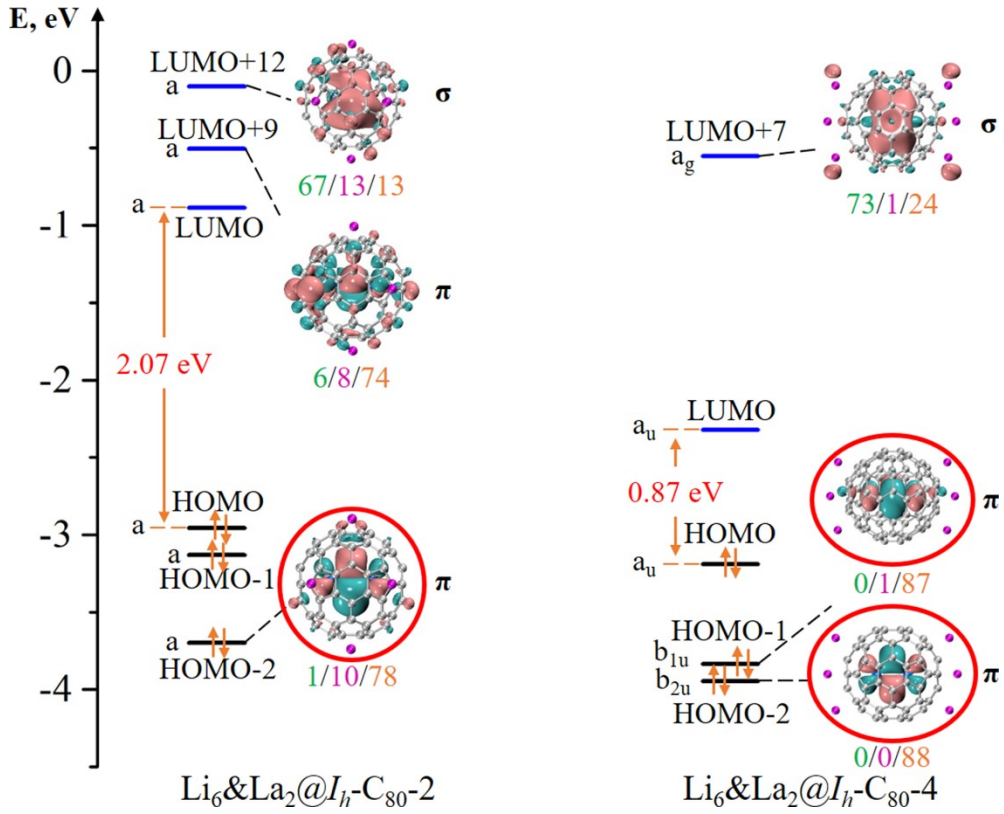

Fig. S13 La-La bonding molecular orbitals of the higher-energy isomers 2 and 4 of $Li_6\&La_2@I_h\text{-}C_{80}$ in Fig. S8 (isovalue: ±0.02 a.u.; occupied and unoccupied orbitals are

denoted by black and blue lines, respectively).

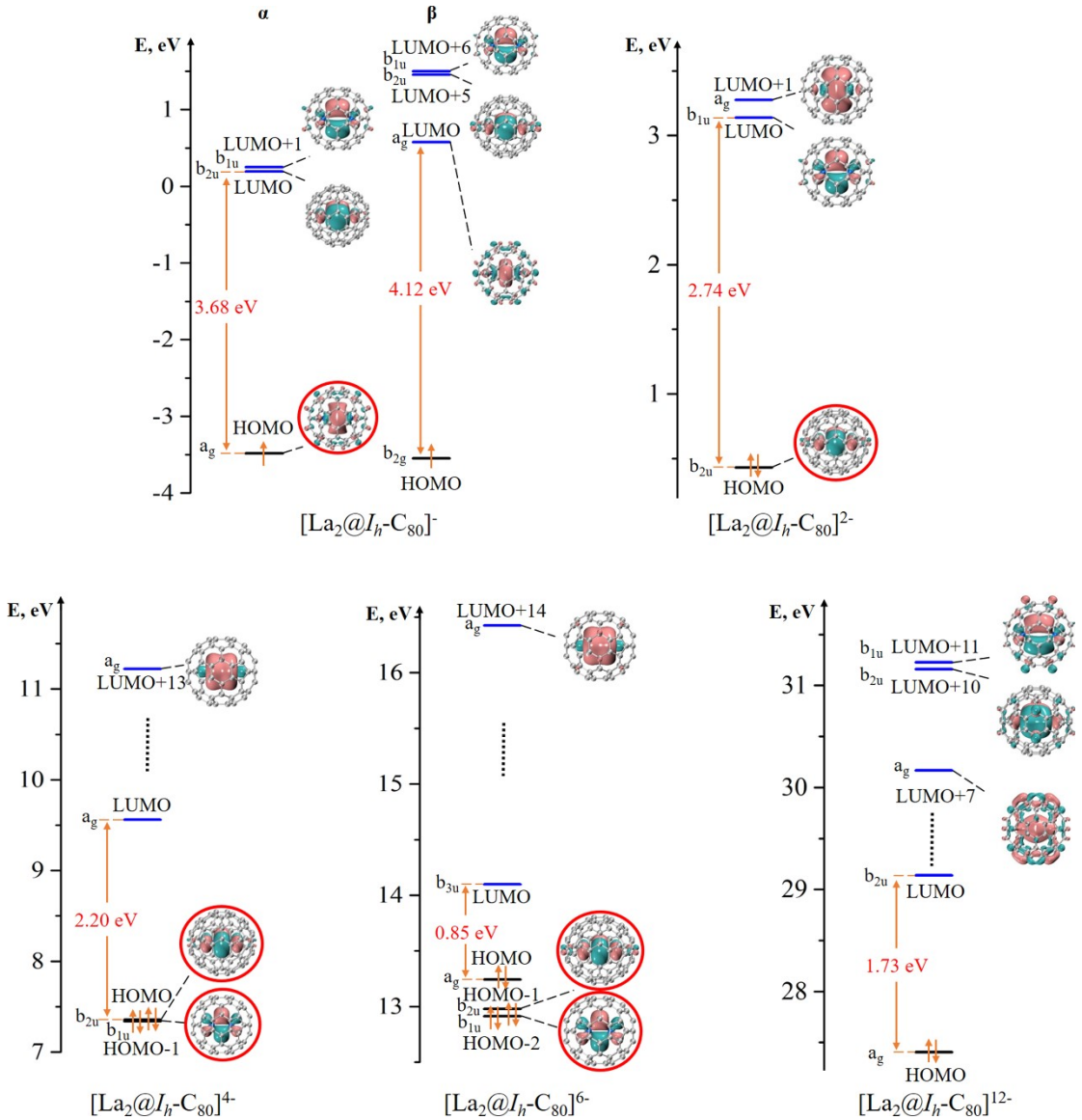

Fig. S14 La-La bonding molecular orbitals of different $[La_2@I_h\text{-}C_{80}]^{q-}$ (q = 1,2,4,6,12) anions (isovalue: ±0.02 a.u.; occupied and unoccupied orbitals are denoted by black and blue lines, respectively).

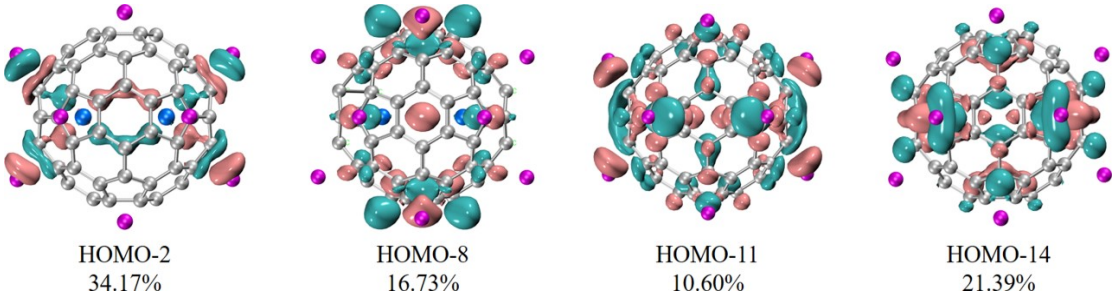

Fig. S15 Occupied frontier molecular orbitals (iso = ±0.02 a.u.) with large metal contributions (% per metal) of Li_{12}&La_2@I_h-C_{80} (D_{2h}).

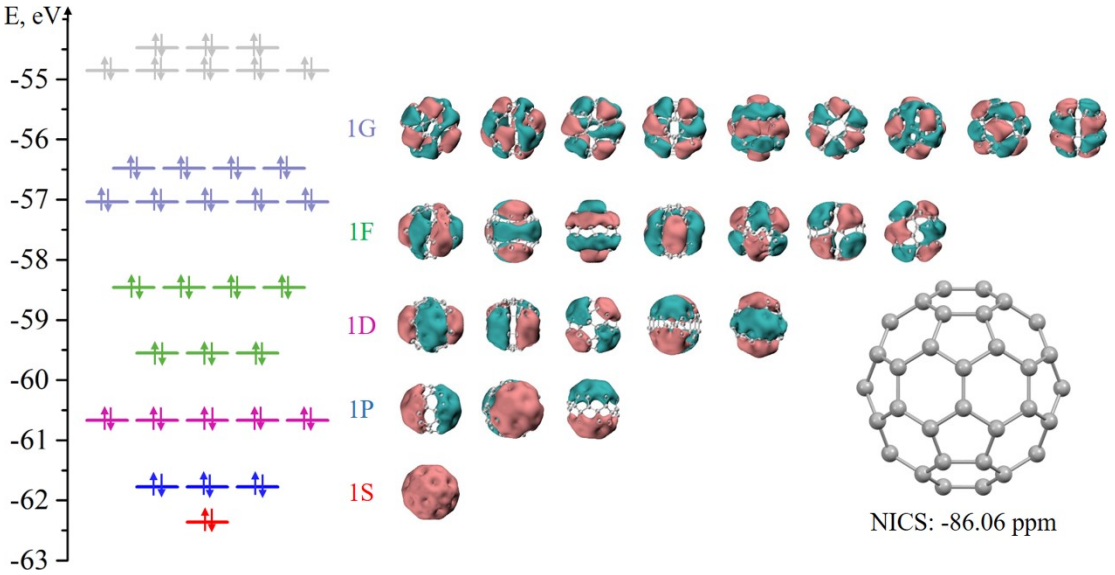

Fig. S16 Optimized structure with NICS value at the cage center and atom-like molecular orbitals of C_{60}^{10+}.

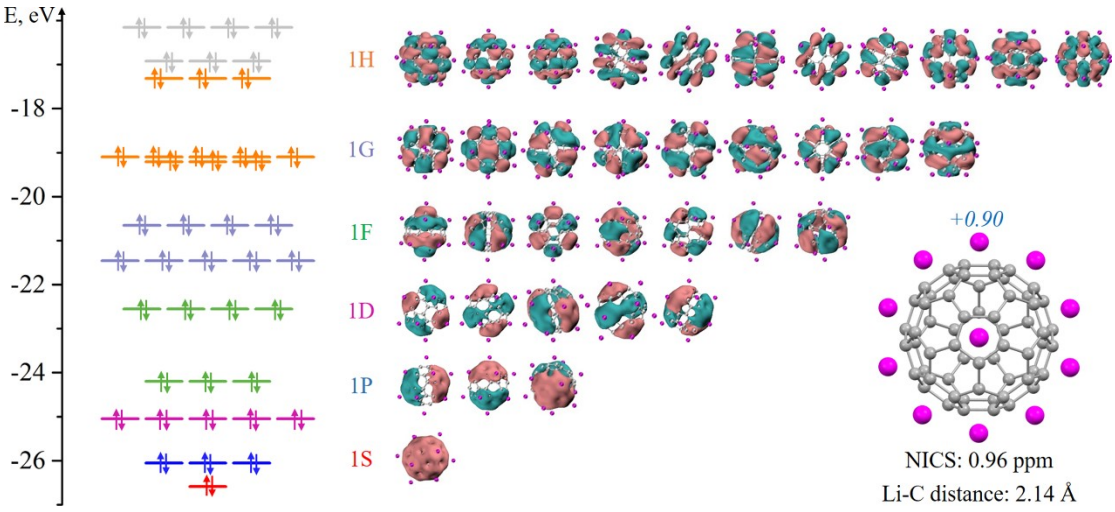

Fig. S17 Optimized structure with NICS value at the cage center and atom-like molecular orbitals of Li_{12}&I_h-C_{60}. The NPA charge of selected Li atom is blue and italic.

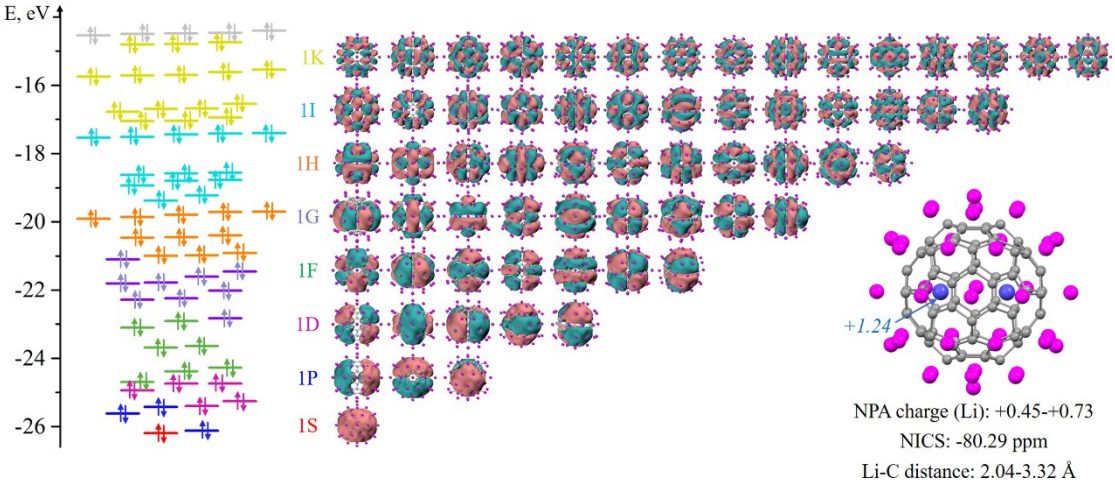

Fig. S18 Optimized structure with NICS at the cage center and atom-like molecular orbitals of Li_{42}&La_2@I_h-C_{80} (D_{2h}). The NPA charge of selected La atom is blue and italic.

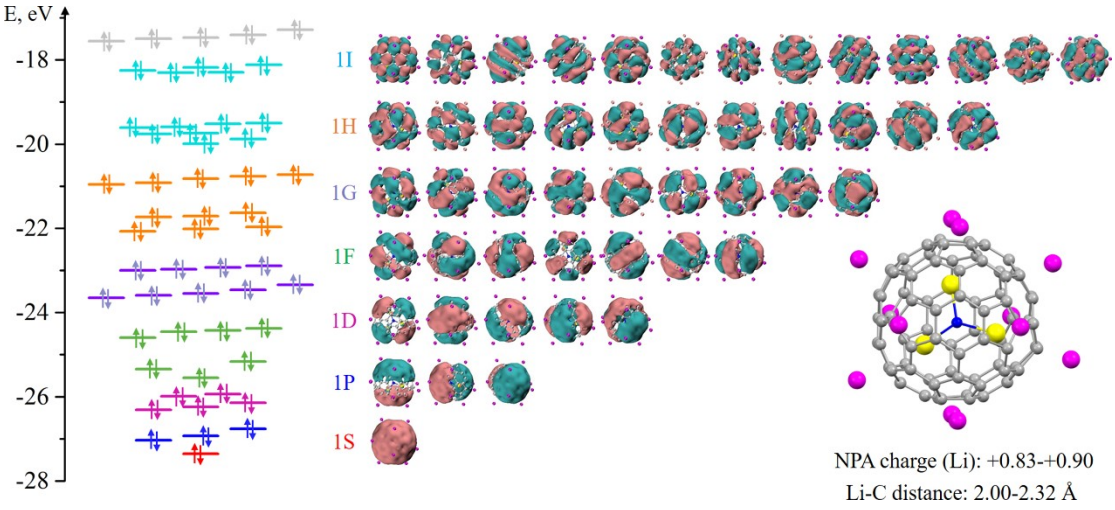

Fig. S19 Optimized structure and atom-like molecular orbitals of Li_{12}&Sc_3N@I_h(7)-C_{80}.

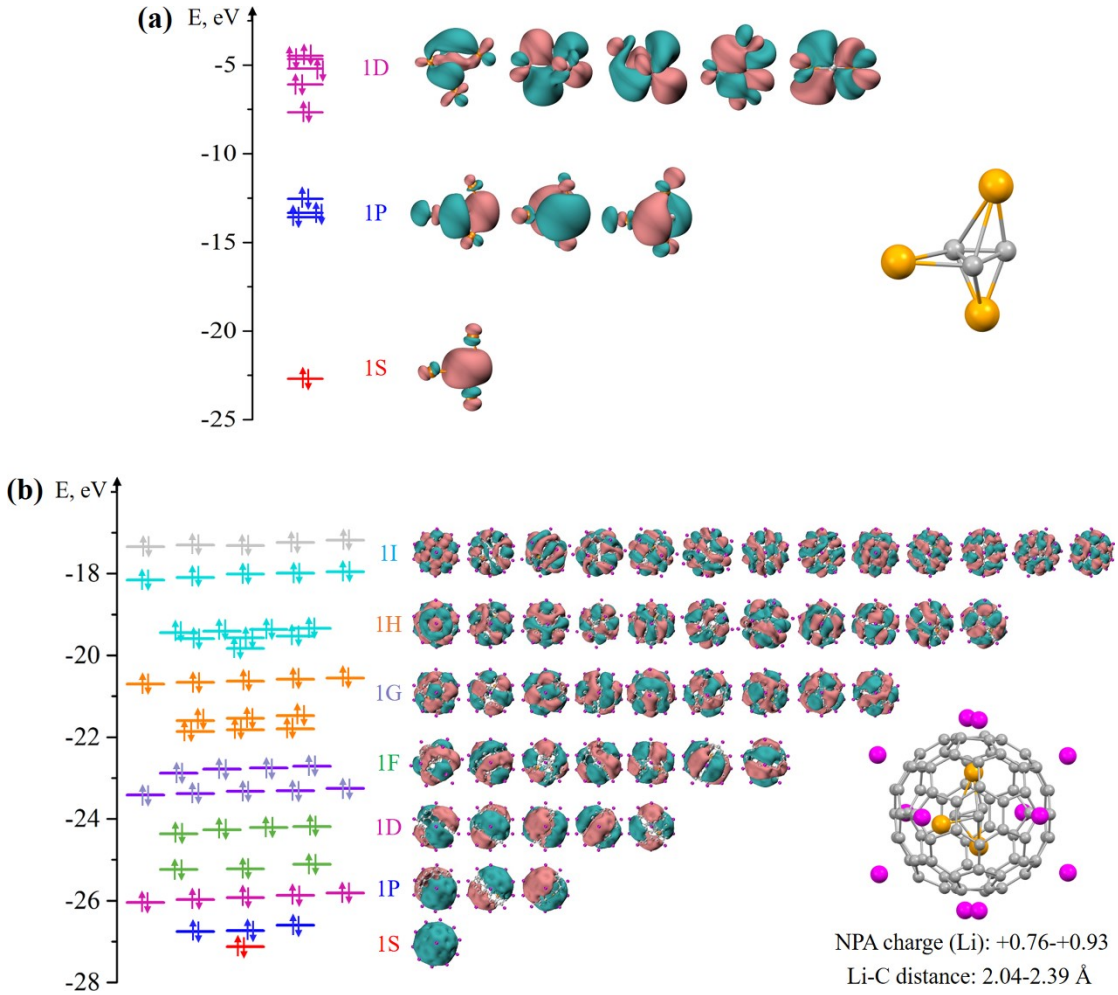

Fig. S20 (a) Nine atom-like molecular orbitals of the internal $(Ti_3C_3)^{6+}$ unit in $Ti_3C_3@I_h(7)$-C_{80}; (b) optimized structure and atom-like molecular orbitals of Li_{12}&$Ti_3C_3@I_h(7)$-C_{80}.